

Morphology and electro-optic properties of polymer-dispersed liquid-crystal films

Karl Amundson, Alfons van Blaaderen,* and Pierre Wiltzius

Bell Laboratories, Lucent Technologies, 600 Mountain Avenue, Murray Hill, New Jersey 07974

(Received 12 September 1996)

An attractive way of making polymer-dispersed liquid-crystal (PDLC) films is through photopolymerization-induced phase separation. The electro-optic properties of these films are determined in large part by the size, shape, and packing of the embedded liquid-crystal drops. We explore the relationships between the conditions of phase separation, morphology, and electro-optic properties. A strikingly strong dependence of electro-optic properties on the fraction of liquid crystal in the film is demonstrated and explained by consideration of the phase separation process. Also, confocal microscopy is shown to be a useful, noninvasive means of obtaining three-dimensional information on PDLC morphology. Not only does it provide very clear images of liquid crystalline drops in the film, but unexpected features were revealed. The drops exhibit a morphology much like a polyhedral foam in the films studied. Polymeric filaments inside the drops were observed as well as a drift in the average size of the drops with proximity to the film substrates. All of these features have important consequences for the electro-optic performance of PDLC films. [S1063-651X(97)13302-5]

PACS number(s): 61.30.-v, 42.70.Df

I. INTRODUCTION

Liquid crystals are used as electro-optic materials in a variety of applications. Thin films of nematics between conductive substrates, for example, are widely used in “twisted-nematic” and “supertwisted-nematic” flat-panel displays. Over the past decade, several new dispersions of liquid crystals and polymers have been developed. One of these is the polymer-dispersed liquid crystal (PDLC), where the liquid crystal is trapped as 1–3 μm diameter drops embedded within a polymeric matrix. PDLCs are candidates for flat-panel displays, switchable privacy windows, and switchable optical elements such as holographic films, because their scattering power can be modulated by an electric field. Typically, as the electric field aligns the liquid crystal in the drops, the scattering power of the film decreases substantially, bringing the film from a highly scattering state to transparency. While twisted- and supertwisted-nematic displays gain their contrast through absorption at polarizers, PDLC films gain contrast through scattering. For this reason, they offer the potential for greater brightness. Electro-optic performance of PDLC films depends strongly upon film morphology. Therefore, an understanding of the relationships between processing, morphology, and electro-optic performance is crucial for controlling film properties.

PDLC films can be made in a variety of ways. Schemes based upon photopolymerization offer simplicity, flexibility, and easy manufacturability. In the simplest scheme, a liquid crystal and a photopolymerizable material are mixed together and then placed between two conductive substrates. Upon UV irradiation the curable component grows in molecular weight and the mixture separates into liquid-crystal-rich drops in a polymer-rich matrix. Coalescence of drops into

very large features is arrested by solidification as the matrix crosslinks.

This paper discusses the relationship between parameters of preparation and morphology for a particular PDLC system. Trends, including the very strong dependence of drop size on small changes in composition, are explained based upon the phase behavior of the precursor materials. Also, we introduce the use of fluorescence confocal optical microscopy for the nondestructive study of PDLC morphology. Fluorescence confocal microscopy is well suited for the study of the three-dimensional structure of PDLC films for several reasons. Most importantly, with confocal microscopy thin optical sections, on the order of 500 nm thick, can be obtained with an in-plane resolution that is higher than with conventional microscopy (about 200 nm). By limiting the field of view to a diffraction-limited spot and imaging the fluorescent light onto a point detector, essentially all out-of-focus light that contributes to an image taken with a conventional microscope is rejected and an increased resolution is obtained [1]. Digital image analysis on a stack of such optical sections can be used to analyze the structure in three dimensions. The use of incoherent fluorescent light reduces the chance of artifacts due to interference effects. Several striking and unexpected features are revealed in this investigation.

II. EXPERIMENT

A series of PDLC films was made using mixtures of a UV-curable material (PN393) and a liquid-crystal mixture (TL205), both supplied from E. Merck (Darmstadt). PN393 is a mixture of acrylate monomers that forms a cross-linked network upon curing with ultraviolet light. TL205 is a mixture of halogenated bi- and ter-phenyls with aliphatic tails of lengths two to five carbons [2]. The pseudobinary phase behavior of the liquid crystal (TL205) in precured PN393 was determined by polarized-light optical microscopy with the use of a variable-temperature hot stage. The cloud point was determined upon heating and cooling (0.5 $^{\circ}\text{C}/\text{min}$) for sev-

*Present address: Van 'tHoff Laboratory for Physical & Colloid Chemistry, Utrecht University, Padualaan 8, 3584 CH Utrecht, The Netherlands.

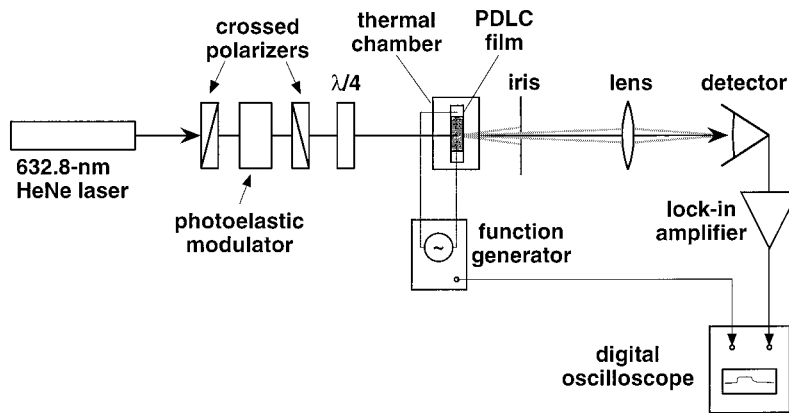


FIG. 1. Electro-optic apparatus for measuring forward light transmission through PDLC films. Light scattered outside a cone with a 1° half-angle is blocked by the iris.

eral compositions. Filtered green light was used to avoid photopolymerization during observation.

PDLC films were made by placing mixtures of the two fluids in a thin gap between indium-tin-oxide-coated glass plates, then curing with ultraviolet (UV) light. For confocal microscopy, the mixtures contained a small amount (ca. 10^{-2} wt%) of dye (BODIPY; Molecular Probes Inc., Eugene, Oregon, or Pyrromethene 580; Exciton Chemical Co., Dayton, Ohio). The dyes give contrast for fluorescence microscopy by selectively staining the polymer-rich matrix of resulting PDLC films. A cell gap of about $14 \mu\text{m}$ was maintained with glass microsphere spacers. The films were then cured by UV irradiation from a Hg-arc lamp with dichroic filters to attenuate light with wavelengths far from 365 nm. The irradiation intensity was 17 mW/cm^2 and the irradiation time was greater than eight minutes to insure full cure.

Another PDLC film was made from a mixture of TL205 with a UV-curable mixture containing 85 wt% lauryl acrylate, 13.5 wt% trimethylol propane triacrylate (to introduce cross-linking to the matrix) and 1.5 wt% photoinitiator. The liquid-crystal fraction in the mixture was 77 wt%. The compositions were chosen so that the resulting PDLC films have a typical drop size similar to those made using PN393 with 80–82 wt% liquid crystal.

Electro-optic properties of PDLC films were measured by use of the apparatus shown in Fig. 1. Helium-neon laser light, propagating normal to the plane of the PDLC film, first was modulated at 100 kHz by a photoelastic modulator between crossed polarizers, then made circularly polarized by a quarter-wave plate. The collection half-angle for the transmitted light was set to 1° by an iris. The forward-transmitted light was then focused by a lens onto a photodetector. The photodetector signal was amplified and demodulated by a lock-in amplifier, which used the photoelastic modulator signal as a reference. (In this manner, background light was eliminated from the measurement.) The signal from the lock-in amplifier was recorded by a digital oscilloscope.

A gated, 1 kHz, sinusoidal voltage was applied to the PDLC film. The pulse duration was 500 ms, or longer when dictated by the relaxation time of the film. The voltage amplitude was varied in consecutive experiments; the transmitted light intensity and the response times (both rise and fall) were measured. V_{90} is the voltage required to bring the film through 90% of the change in transmittance from the “off” (zero field) state to the ultimate transmittance at high voltage. Rise and fall times are defined as the time interval be-

tween 10% to 90%, or 90% to 10%, respectively, of the total change between the “on” and “off” transmittances.

The fluorescence confocal micrographs were made using a Multiprobe 2001 confocal setup of molecular dynamics and a $100\times$ oil 1.4 numerical aperture lens on an inverted Nikon Diaphot microscope. The dye BODIPY or pyrromethene was excited at 514 nm and fluorescent light above 535 nm was detected. A voltage sufficient to align the nematic texture in the PDLC film was applied to the films during confocal microscopy. This minimized the loss of intensity and distortion of the imaging and fluorescent light due to scattering from the PDLC structure. Depth corrections for the slight difference in refractive index of the immersion oil (1.52) and the switched film were made assuming an index of refraction of 1.51. Optical sections in the “ x - y ” plane (parallel to the film substrates) had 512×512 pixels with a lateral pixel dimension of 63 nm. “ Z ” sections, perpendicular to “ x - y ” sections, had a vertical pixel size of 100 nm.

III. RESULTS AND DISCUSSION

A. Electro-optic properties

The electro-optic properties of PDLC films made from mixtures of TL205 and PN393 depend upon several parameters of preparation, including the liquid-crystal fraction,

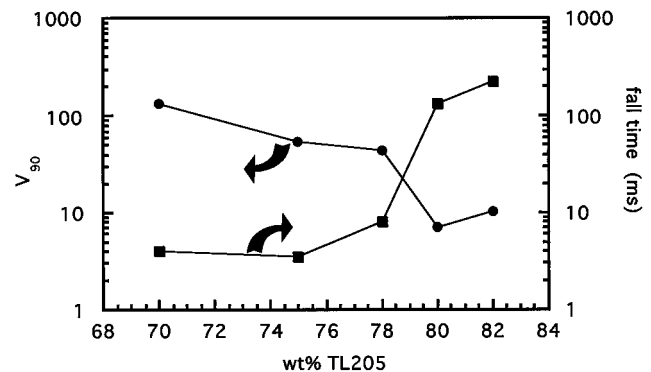


FIG. 2. V_{90} and fall time (after cessation of voltages greater than V_{90}) as a function of the weight fraction of TL205. V_{90} for the film with 70 wt% TL205 exceeded the breakdown voltage, and was estimated by superposition of the partial transmittance-voltage curve onto complete curves for films with lower switching voltages. Also, the fall time for that composition was taken at the largest voltage tested, and not at voltages above V_{90} .

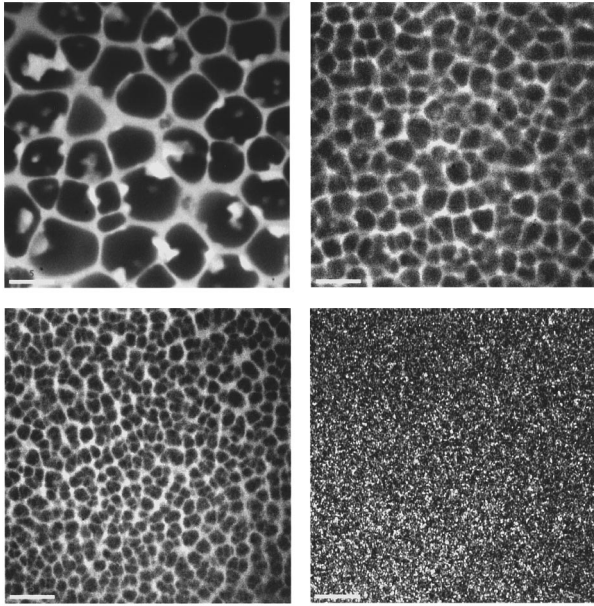


FIG. 3. Confocal microscopic “x-y”-section images of PDLC films made from TL205 and PN393. All images were collected near the midplane of the films. The liquid-crystal fraction is (a) 82 wt %, (b) 80 wt %, (c) 75 wt %, and (d) 70 wt %. The texture in (d) is due to noise. The scale bar indicates 5 μm .

temperature during cure, and cure rate. Perhaps the most striking effect is the very strong dependence of properties on the liquid-crystal fraction. Figure 2 shows the switching voltage, V_{90} , and the relaxation time as a function of the liquid-crystal fraction. All other conditions of preparation were kept constant, including the temperature during cure of 22 $^{\circ}\text{C}$. V_{90} changes by about a factor of 20, and the fall time by almost 100 across the full experimental range, with most of the changes occurring across the rather small range of 77–80 wt% liquid crystal. In this section, this very strong dependence is explored.

Confocal microscopic images of a series of PDLC films made from mixtures of TL205 and PN393 reveal a “polyhedral foam texture” morphology and a rapidly increasing average drop size with an increasing liquid-crystal fraction, as can be seen in Fig. 3. For films made from mixtures of 72 wt % or less liquid crystal, no structure was observed, presumably because the features are smaller than the 0.2 μm resolution limit of the microscope. The inverse square root of the number of drops intersecting the image plane divided by the image area

$$\langle L \rangle = \left[\frac{(\text{image area})}{(\text{number of drops})} \right]^{1/2} \quad (1)$$

is graphed in Fig. 4 as a function of composition. This quantity scales approximately with the drop size, and is on the order of the drop diameter.

The increase in drop size with an increasing liquid-crystal fraction leads to a decreasing switching voltage and increasing fall time with increasing liquid-crystal fraction. A semi-quantitative argument based upon consideration of elastic distortion energy and electric field energy gives a switching voltage according to [3–5]

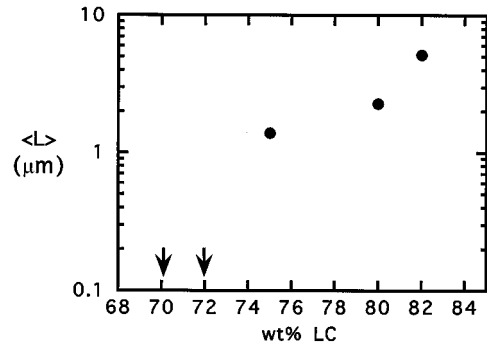


FIG. 4. The inverse square root of the number of drops in the confocal image divided by area. This number scales roughly with the average drop diameter. The arrows indicate that the drop size is below the resolution limit of the microscope for the films made with 70 and 72 wt % liquid crystal.

$$V_{\text{switch}} \approx \frac{1}{c} \frac{d}{R} (\mathcal{L}^2 - 1) \left(\frac{4\pi K}{\Delta\epsilon} \right)^{1/2}, \quad (2)$$

where R is a characteristic drop radius, d the film thickness, and \mathcal{L} the ratio of the largest to the smallest radii, assuming the drops to be ellipsoidal. K is the nematic elastic constant, and $\Delta\epsilon$ is the dielectric anisotropy of the liquid crystal. The prefactor c^{-1} represents the field-gathering effect due to a dielectric or conductivity mismatch between the drops and the surrounding matrix.

The relaxation time of the nematic director in a drop can be approximated by balancing the driving force toward relaxation against viscous dissipation

$$\tau_{\text{OFF}} = \frac{\gamma_1 R^2}{K(\mathcal{L}^2 - 1)}, \quad (3)$$

where γ_1 is a rotational viscosity coefficient. Presuming the drop shapes are similar in the series of films, Eqs. (2) and (3) predict that the switching voltage will decrease and the relaxation time increase as the drop size increases. Indeed, this is born out by comparison of Figs. 2 and 3. It should be noted that these arguments are based upon the assumption of strong anchoring of the liquid crystal at the drop surfaces, and this is not necessarily the case. Surface anchoring in these materials is the subject of a separate report [6].

The physical and chemical processes associated with photopolymerization-induced phase separation are numerous and complex. But through consideration of the phase separation process, the strikingly strong dependence of electro-optic properties and film morphology on the liquid-crystal fraction can be rationalized.

The pseudobinary phase behavior of uncured TL205-PN393 mixtures is shown in Fig. 5. Cloud points measured by polarized-light microscopy (average for heating and cooling) are shown. The lines separate the parameter space into a single-phase isotropic, single-phase nematic, and a biphasic region. The qualitative character of the phase diagram has been reported previously for mixtures of liquid-crystal and photocurable materials [7–9]. The two-phase region can be understood as a hybrid of the typical two-phase envelope for simple liquids and, in the high liquid-crystal fraction region,

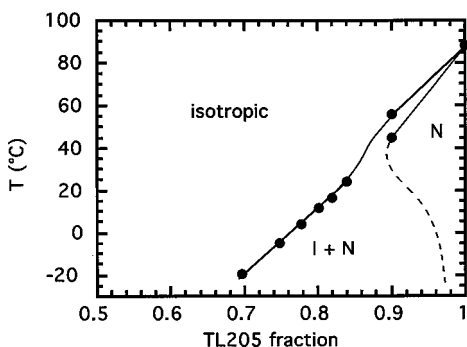


FIG. 5. Phase behavior of the uncured TL205-PN393 mixture as determined by polarized-light microscopy. Solid lines connect data points and the dashed curve is a speculative extrapolation. The parameter space is divided into a single-phase isotropic, single-phase nematic (N), and a biphasic ($I+N$) region.

a nematic-isotropic transition that opens up to a biphasic region due to addition of a non-nematic constituent (PN393).

It is important to be aware of conceptual limitations in the use of binary phase diagrams for this system. Both the liquid-crystal and the photocurable mixture contain several components. The binary phase diagram is useful only to the degree that each material acts as a single phase. It cannot be extended to include phenomena such as preferential solubility of one component of the liquid-crystal mixture into the PN393, for example. Elastic forces emerging beyond the gel point of the polymeric component require additional considerations. The phase diagram is used here because it offers great simplicity and is sufficient to explain several phenomena early in the phase separation process.

Upon UV irradiation, the increase in molecular weight of the acrylate component results in an expansion of the two-phase envelope [see Fig. 6(a)], primarily because of a reduction in the entropy of mixing. (The only stationary point is the nematic-isotropic transition temperature of the pure liquid crystal.) After the two-phase envelope rises over the temperature-composition coordinate characterizing the PDLC mixture [see Fig. 6(b)], the mixture phase separates. Because the slope of the coexistence curve is positive at the point where it crosses the temperature-composition coordinate, the minority phase, appearing as drops, is nematic and rich in liquid crystal, in accordance with the lever rule for phase separation. The matrix is non-nematic and rich in polymer. As the coexistence curve moves further upward, the equilibrium volume fraction of the minority phase increases. For this reason, as well as kinetic factors, the drops grow until the matrix becomes sufficiently solid to resist further growth.

It is reasonable to assert that the degree of polymerization, when the drops first form, is an important determiner of drop growth and eventual film morphology. Drop growth requires diffusion of liquid-crystal material towards and diffusion of monomer and polymer away from the drop, and movement of the drop boundary into the polymer-rich region [10]. As the molecular weight of the polymeric component increases, the matrix becomes more viscous and elastic, making growth more difficult. So, in the case where the distance between the coexistence curve and the temperature-composition coordinate is large [point “A” in Fig. 6(b)], the polymerization has

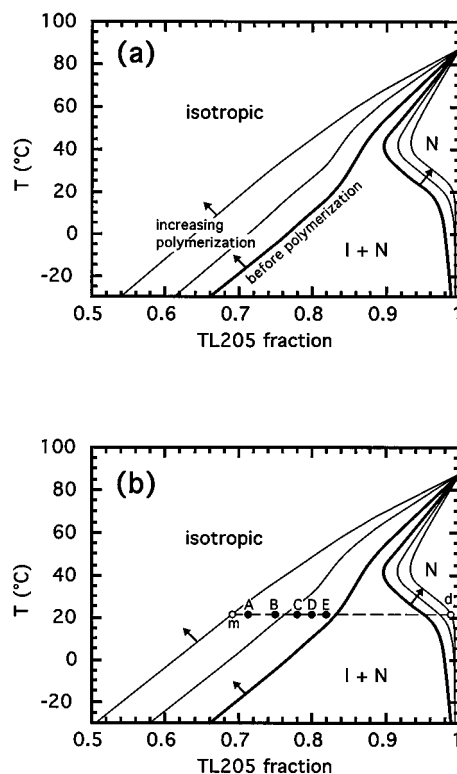


FIG. 6. (a) Binary phase diagram for TL205-PN393 mixtures, and speculative expansion of the two-phase region upon photopolymerization. The coexistence curves, prior to photopolymerization, are indicated by bold lines. As polymerization proceeds the coexistence curves move in the direction of the arrows, as suggested by the (hypothetical) narrow lines. (b) The solid dots are at a set of temperature-composition coordinates characterizing five mixtures used to prepare PDLC films at ambient temperature. Prior to photopolymerization the solutions are single phase and isotropic. Phase separation occurs after the coexistence curve passes over a point; the result is liquid-crystal-rich drops in a polymer-rich matrix whose compositions are indicated by the open circles (denoted by “ d ” and “ m ”, respectively).

proceeded relatively far before phase separation begins, and drop growth is more inhibited than when the liquid-crystal fraction is higher. The resulting slow growth allows time for formation of additional drops in the matrix regions. The result will be a relatively small drop size. If, instead, the temperature-composition coordinate is close to the coexistence curve [point “E” in Fig. 6(b), for instance], phase separation occurs early in the polymerization process. In this case, the growth of drops is relatively fast in this more fluid environment, and the resulting drops are larger. These two situations are contrasted in the illustration of Fig. 7.

This argument leads to the conclusion that, over a limited composition and temperature range, the ultimate film morphology will be determined in large part by the distance between the coexistence curve of the uncured mixture and the temperature-composition coordinate. As a test for this inference, a series of PDLC films was made in the same way as the original set of PDLC films, with the liquid-crystal fraction varying between 70 and 82 weight %. Concurrently, the temperature during photopolymerization was covaried so that the temperature-composition coordinate for each film was 11 °C above the coexistence curve. The coordinates for

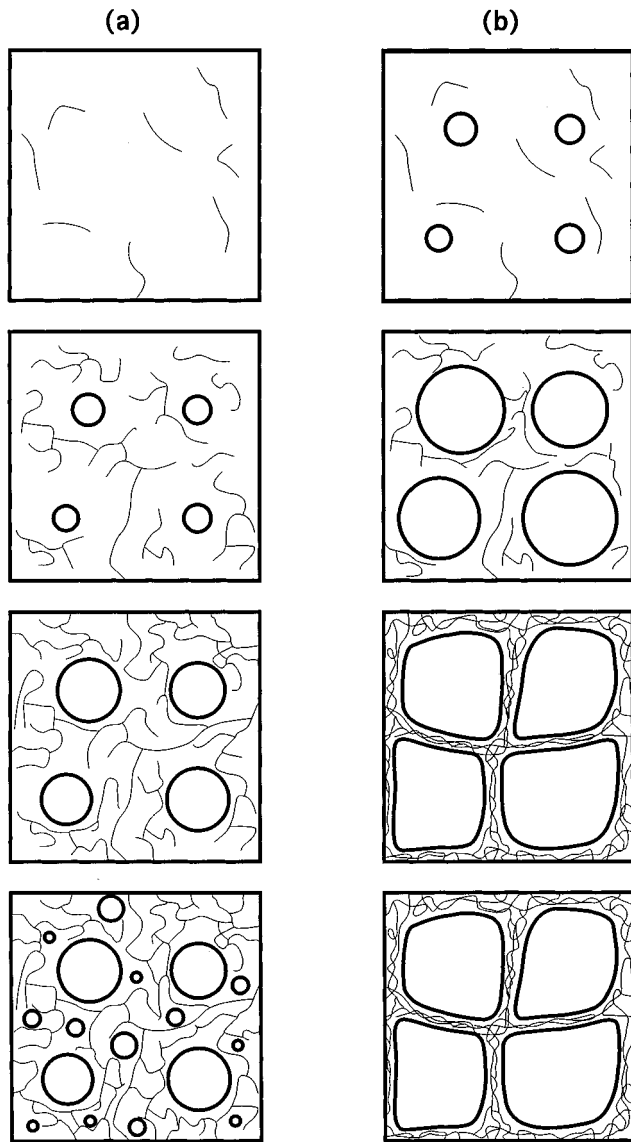


FIG. 7. Phase separation of nematic drops from a polymerizing mixture is illustrated. In (a), the liquid-crystal fraction is relatively low, the drops appear relatively late, and solidification of the matrix resists drop growth. A second generation of drops appears in the last frame. In (b), the liquid-crystal fraction is higher, drops appear earlier, and they grow to fill most of the available space before the matrix is sufficiently solid to resist growth.

these films are shown in Fig. 8. Since the coexistence curve is nearly straight, this maintains a uniform distance between the curve and each coordinate. By optical microscopy the characteristic drop size was found to vary much less than in the previous set of films that were all prepared at room temperature. The switching voltage and response times at room temperature for the two series of PDLC films are plotted in Fig. 9, along with data from the previous set of films cured at room temperature. The strong composition dependence is greatly attenuated in the set of films cured at conditions equidistant from the coexistence curve. This demonstrates that, at least over a limited range, the distance between the coexistence curve of the uncured material and the temperature-composition coordinate is a strong determiner of the film morphology and electro-optic properties. Changing param-

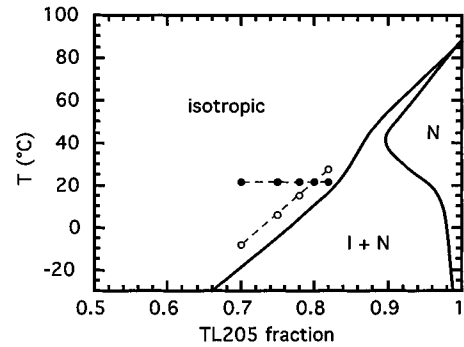


FIG. 8. Temperature-composition coordinates corresponding to the curing conditions of the set of PDLC films cured at ambient temperature are shown by the solid dots. A second set of PDLC films of various composition were cured at temperatures indicated by the open circles. For this set the temperature was set to be 11 °C above the coexistence curve.

eters that cause movement of the temperature-composition coordinate parallel to the coexistence curve has a very small effect on properties, while movement perpendicular to the coexistence curve has a dramatic effect.

From this observation, the strikingly strong dependence of electro-optic properties with small changes in composition can be easily understood. The important parameter to consider is not the liquid-crystal fraction, f_{LC} , but the difference between the liquid-crystal fraction and the saturation value at the temperature during curing, $f_{LC,sat} - f_{LC}$. It is this parameter that changes strongly with very small changes in the

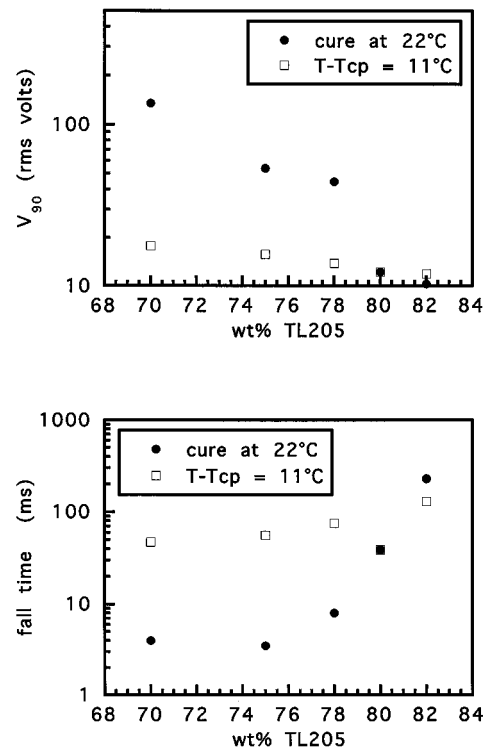


FIG. 9. V_{90} and fall time as a function of the liquid-crystal weight fraction for the set of PDLC films photopolymerized at conditions equidistant from the pre-cured coexistence curve. Also shown are data from the set of films photopolymerized at ambient temperature.

liquid-crystal fraction. For instance, over the composition range 77–80 wt % liquid crystal, very large changes in electro-optic properties were observed. This represents less than a 4% change in f_{LC} , but about a 50% change in $f_{LC,sat} - f_{LC}$.

Finally, it is reasonable to expect that the observations here could be quite general to other PDLC systems, as the arguments are based on the phase behavior of the two materials, and this behavior should be quite general. The strong dependence of morphology and electro-optic properties on composition in the system studied here is related to the large slope of the coexistence curve near the curing conditions (300 K⁻¹). The dependence on composition should be less for other mixtures where this slope is smaller and vice versa. Another prediction is that the temperature dependence should follow a reciprocal relationship. That is, when the slope of the coexistence curve is high, the dependence of properties on the temperature during cure should be small, and when the slope is low, the dependence on temperature high. It would be interesting to test these predictions on a number of related systems.

B. General morphological features

The preceding section showed how fluorescence confocal microscopy is a very useful, noninvasive method for observing PDLC film morphology, at least for structures greater than the resolution limit of about 0.2 μm in the lateral directions, and 0.5 μm in the vertical direction. In addition to revealing the size and shape of drops, several unexpected and important morphological features were observed using confocal microscopy. They, and their importance to electro-optic performance, are described next.

1. Polyhedral foam texture morphology and its ramifications

The TL205-PN893 films exhibit a polyhedral foamlike microstructure in many respects (Fig. 3). The drops are tightly packed and distorted in order to accommodate each other's presence, and the matrix is confined to relatively thin walls between the drops. The drop cross section, characterized by sharp vertices between flat interfacial regions and the relatively thin walls between the drops, gives the morphology a similarity to polyhedral foams. This is quite distinct from the commonly observed "Swiss cheese" morphology, where the drops are well separated by the matrix and are more spherical.

"Polyhedral foam texture" morphologies are also attained when a wide variety of alkyl acrylate mixtures are used in place of PN393. For instance, a mixture we used is comprised of ~85 wt % monofunctional alkyl acrylate, ~14 wt % trifunctional acrylate, and ~1% photoinitiator. It is likely that the polyhedral foam texture morphology results from the low functionality of the acrylate mixtures as well as the high liquid-crystal fraction. The high liquid-crystal fraction allows the drops to fill most of the available space as long as the matrix remains sufficiently fluid during drop growth. A high functionality matrix would cross-link, and thus solidify, much earlier in the process of phase separation.

The polyhedral foam texture morphology has quantitative as well as qualitative ramifications for the properties of PDLC films. Light scattering from PDLC films is often un-

derstood in terms of a field-modulated scattering cross section for the drops in the film [1,12]. The ordinary refractive index of the liquid crystal and the refractive index of the polymer matrix are chosen to match so that when the texture inside each drop is aligned by the electric field, the scattering cross section is low (at least for light of normal incidence whose electric field sees only the two matched refractive indices). In the "off" state (no applied field), the texture in each drop is oriented in some other direction, the electric field of light may experience the extraordinary refractive index of the liquid crystal, and so the average drop scattering cross section is large. There can be additional scattering from the spatial variation in the dielectric tensor inside the drops due to curvature of the director field.

By making the first Born approximation, where only single scattering events are considered, the electric field of the scattered light is given by $\mathbf{A}_{sc}^{(1)}/r$, where

$$\mathbf{A}_{sc}^{(1)}(\mathbf{k}') = \frac{k^2}{4\pi} \int d^3x \frac{\underline{\underline{\epsilon}}}{\epsilon_0} \cdot \mathbf{D}_0 e^{i(\mathbf{k}-\mathbf{k}') \cdot \mathbf{x}} \quad (4)$$

and r is the distance from the observation point to the scattering position. \mathbf{k} and \mathbf{k}' are the incident and scattered wave vectors, $\underline{\underline{\epsilon}}$ the spatially varying dielectric tensor, and ϵ_0 the space average of $\underline{\underline{\epsilon}}$. \mathbf{D}_0 is the electric displacement field of the incoming wave.

From this equation, it can be seen that light is scattered from components of $\delta\epsilon$ with wavelengths on the order of the wavelength of light (so that the integrand is slowly varying). In a PDLC film, several contributions are (1) the contrast between the polymer matrix and liquid crystal, (2) variations within drops, and (3) contrast between neighboring drops.

The first two contributions are present even when the drops are separated by large distances. They are most important in PDLC films with the Swiss cheese morphology. But, when the drops are more tightly packed, as in the polyhedral foam texture morphology, the interdrop contrast becomes increasingly important. The concept of a scattering cross section for a single drop loses meaning and one must speak about the scattering power of the ensemble as a whole.

Drzaic [13,14] studied the effect of the drop number density on scattering power in PDLC films made by an emulsion method. Drzaic interpreted his results in the framework of anomalous diffraction theory, and showed that the scattering efficiency of drops in the field-aligned state decreased with increasing crowding of drops. This is evidence that at high drop densities the interdrop contrast is a critically important factor. Here, we arrive at a similar conclusion although from different experiments.

To test the importance of the interdrop contrast to the scattering power of PDLC films, several films were compressed and sheared. Under either deformation, the scattering power of the films was greatly reduced. In the compression experiment, a portion of the film was compressed, and a region proximate to that portion was studied. There, material was being squeezed away from the region under compression, causing the drops to be elongated in the plane of the film. In the shear experiments, one substrate was pushed past the other, creating a uniform shear deformation. This shear made the drops more prolate, with a long axis oriented between 0° and 45° from the film plane, the angle depending

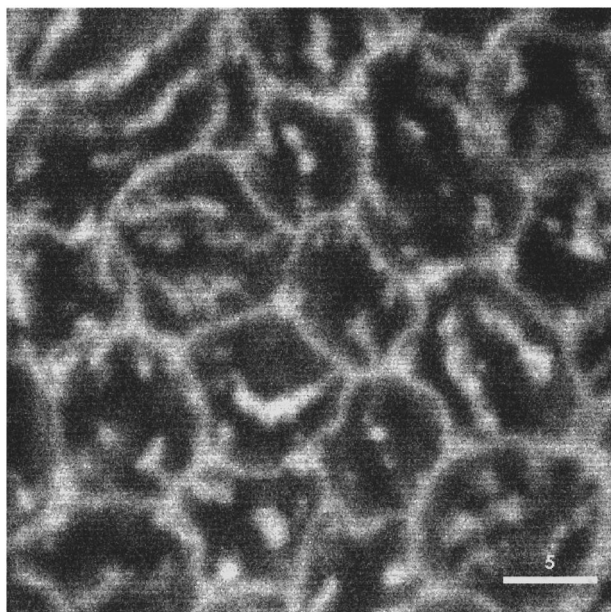


FIG. 10. Confocal microscopic x - y -section image near the midplane of a PDLC film made from 77 wt % TL205 and a lauryl acrylate-based matrix mixture. The scale bar indicates 5 μm .

upon the strength of shear [15]. In the undistorted case, the axis along which the nematic in a drop tends to align is randomly oriented, while either of these distortions will place this axis closer to the substrate plane. This will increase the scattering power of well-separated drops. However, the *interdrop* contrast will decrease because deformation causes the directors in nearby drops to be aligned in the same direction. (This was verified by polarized light microscopy. Specifically, under deformation, the film exhibited a large birefringence, and strong extinction when the deformation axis was aligned with either the polarizer or analyzer.) The large decrease in the film scattering power with deformation argues that the interdrop contrast is a dominant contributor to the film scattering power in the zero field state. Our interpretation is that drops are separated by a distance small or on the order of the wavelength of light, so that it is the contrast between the drops that is a more significant contributor to scattering than the contrast between drops and the polymer matrix. The dominance of interdrop contrast is the basis for the low “off-angle haze” exhibited by these films. Light of oblique incidence will experience a more spatially uniform effective dielectric constant when the nematic in the drops is aligned uniformly by the field and the matrix component is minimized.

2. Polymer filaments in drops

Many of the drops in the PDLC films studied contain polymeric globules. Some are apparent in the three sets of confocal images in this paper. Examination of transverse sections at various depths through the film reveals that these globules are typically extended, or filamentary, and usually join with drop surfaces. They are observed in PDLC films made from TL205 and various acrylate-based matrix materials, including PN393. These features appear more prevalent

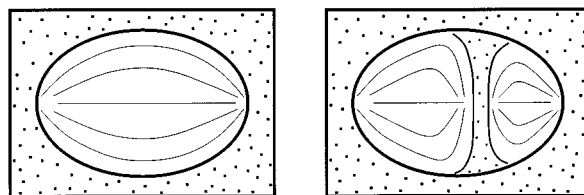


FIG. 11. An illustration showing the effect of a polymer filament on the director field pattern within a drop.

in larger drops, and exist in a majority of the drops that are on the order of or larger than $\sim 3 \mu\text{m}$. They are less apparent in films with smaller drops, but that may be partly due to the difficulty in observing small features.

In the PDLC film made using the lauryl acrylate-based matrix (see Fig. 10), the filaments are numerous (several per drop), consistent with the large drop size, and their cross section is typically extended with a long direction parallel to the nearest portion of the wall. In addition, many of the walls have breaks, so that the distinction between “filaments” and broken walls is less clear. The origin of these structures is not apparent. Perhaps they form when the less viscous liquid crystal displaces the more viscous (and elastic) matrix during phase separation and drop growth. Polymer filaments that are sufficiently solid may be left behind by the advancing liquid-crystal front.

Certainly the nematic director field in a drop will be disturbed by the presence of polymer filaments, as illustrated in Fig. 11. The additional surfaces and associated surface anchoring imposed by the filaments will sharpen the nematic curvature and increase the nematoelastic distortion energy inside the drop. The voltage required to switch the texture will then be greater, and the film will relax faster. The effect on the scattering power of the film depends upon the drop size. If drops are much larger than the wavelength of light, the stronger nematic curvature due to filaments in the drops will increase scattering power. But, if the drops are smaller than the wavelength of light, the filaments will widen the distance between the wavelength of light and the nematic curvature, thus decreasing the scattering power of the film.

3. Variation in morphology with proximity to the film-substrate interface

The morphology of the films surveyed are not uniform throughout the film, but instead vary with proximity to the film-substrate interfaces. Broad generalizations from our observations are not forthcoming, but several significant observations are reported here. The most general observation is that the drop size tends to decrease with proximity to the film-substrate interfaces. An example is shown in Fig. 12, and the number of drops that intersect each of the image planes is shown in Fig. 13. Confocal images at intermediate positions show a gradual evolution of the average drop size across the film. There is a striking break in reflection symmetry across the film midplane, which is common but not always reproducible. Gravity is a symmetry-breaking agent, as the density of the liquid crystal is 1.20 g/cm^3 and the

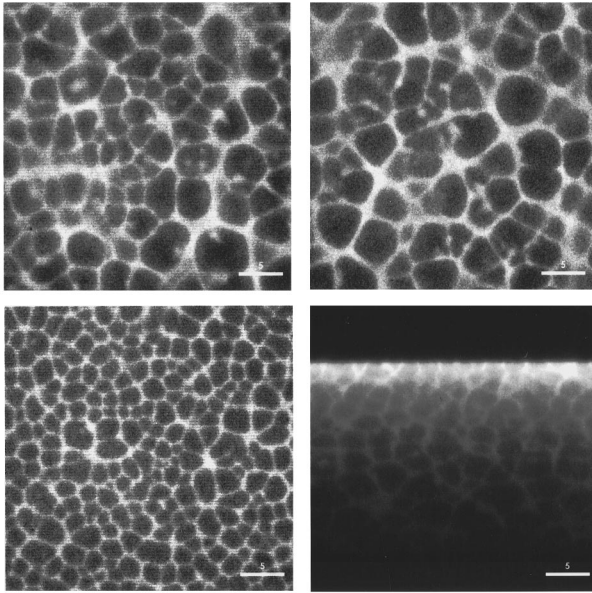


FIG. 12. Confocal microscopic x - y -section images of a $20\ \mu\text{m}$ thick PDLC film made from TL205 and PN393, with 80 wt % TL205. The first three images were taken (a) one micrometer from the top surface, (b) at the midplane, and (c) one micrometer from the bottom surface. (d) shows a z section through the film.

monomer has a density of $0.90\ \text{g}/\text{cm}^3$. Sedimentation of drops during photopolymerization in the system under study has been observed using microscopy [10].

By balancing viscous drag force ($12\pi\eta vR$) against buoyancy ($4\pi R^3\Delta\rho g/3$), a rough estimate of the sedimentation velocity is given by

$$v = \frac{\Delta\rho g R^2}{9\eta}, \quad (5)$$

where η is the viscosity of the surrounding fluid, v the sedimentation velocity, R the drop radius, $\Delta\rho$ the drop density minus the solution density, and g the acceleration of gravity. This approximation ignores several important factors including the proximity of drops, internal flow within the drops, the rapidly increasing viscosity and elasticity of the matrix, and possible electrostatic interactions between drops or drops and the substrates.

If the time between drop formation and the matrix solidification is given as Δt , then Eq. (5) gives a vertical displacement of the drops as

$$\Delta x = \frac{\Delta\rho g R^2}{9\eta} \Delta t. \quad (6)$$

Using $\Delta\rho$ of $0.3\ \text{g}/\text{cm}^3$, $R \sim 1\ \mu\text{m}$, $\eta \sim 0.027\ \text{g}/\text{cm s}$ [16], and $\Delta t \sim 3\ \text{s}$ [10], $\Delta x \sim 0.4\ \mu\text{m}$. This estimate is on the order of the typical drop radius, but about an order of magnitude smaller than the thickness of the cell gap. Because of the severe approximations made, this calculation does not rule out the possibility of gravitational forces inducing sedimentation of drops during photopolymerization.

The other common observation is a reduced drop size near the substrates compared to those in the middle of the

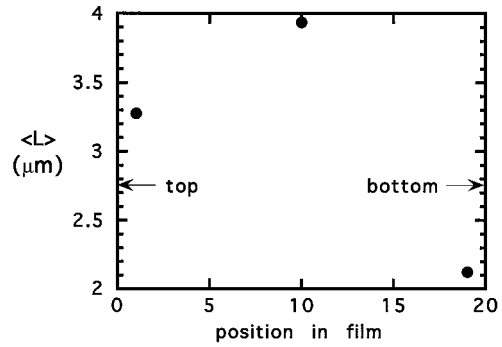


FIG. 13. The inverse square root of the number of drops in the confocal image divided by area. This number scales roughly with the average drop diameter. The top and bottom substrates, defined by the orientation of the film during photopolymerization, are at zero and $20\ \mu\text{m}$, respectively.

films, as shown in Figs. 12 and 13. Drops can gain liquid-crystal material only from the surrounding fluid and not the substrates. Therefore, transport of material to and away from drops near a substrate is limited by proximity to the substrate. They will grow more slowly than those in the central region of the film.

Nonuniformity in drop size across the thickness of a film is important because the drop size affects the scattering power, switching voltage, and response time. For example, the drop size nonuniformity will broaden the transmittance versus voltage curve. With an increasing field, the region near the film midplane, with larger drops, will become clear first, and the regions near the substrates, with smaller drops, will become clear at a higher field.

IV. CONCLUSIONS

The relationship between the liquid-crystal fraction and temperature during curing on the morphology and electro-optic properties of a photopolymerized PDLC film has been studied. A strikingly strong dependence of properties on the liquid-crystal fraction was explained by consideration of the phase separation process. An important parameter is the distance between the temperature-composition coordinate and the coexistence curve, and this parameter changes rapidly for small changes in liquid crystal fraction in the vicinity of the coexistence curve. More generally, rapid changes occur for movement of the temperature-composition coordinate toward or away from the coexistence curve, and changes are very mild for transverse movement of this coordinate. It was argued that the physical basis for these trends does not depend upon specific details for the system studied, but is quite general for photopolymerized PDLC films. A prediction is that the sensitivity to composition and temperature for a given mixture will be related to the slope of the coexistence curve near the photopolymerization conditions.

Confocal microscopy is a useful, noninvasive means of obtaining three-dimensional information on PDLC morphology. Not only does it provide very clear images of the drop size and shape, but unexpected features were revealed. PDLC films made from TL205 and a variety of alkyl acrylate matrices exhibit a ‘‘polyhedral foam texture’’ morphology,

where the drops are tightly packed and separated by thin polymeric walls. It was shown that interdrop contrast is a primary scattering mechanism, and this is a likely reason for the relatively low off-angle haze seen in these films. Polymer filaments inside drops were prevalent in many films, and the average drop size was found to vary with distance from the substrates.

ACKNOWLEDGMENTS

Alfons van Blaaderen received support for this work through the research program of the Dutch Organization for Fundamental Research on Matter (FOM) and was made possible by financial support of the "Nederlandse Organisatie voor Wetenschappelijk Onderzoek" (NWO).

-
- [1] Confocal Microscopy, edited by T. Wilson (Academic, London, 1990).
- [2] Dr. David Coates (private communication).
- [3] P. S. Drzaic and A. Muller, *Liq. Cryst.* **5**, 1467 (1989).
- [4] B.-G. Wu, J. H. Erdmann, and J. W. Doane, *Liq. Cryst.* **5**, 1453 (1989).
- [5] K. Amundson, *Phys. Rev. E* **53**, 2412 (1996).
- [6] K. Amundson and M. Srinivasarao (unpublished).
- [7] G. W. Smith, *Mol. Cryst. Liq. Cryst.* **196**, 89 (1991).
- [8] G. W. Smith, *Phys. Rev. Lett.* **70**, 198 (1993).
- [9] Y. Hirai, S. Niiyama, H. Kumai, and T. Gunjima, *Rep. Res. Lab. Asahi Glass Co.* **40**, 285 (1990).
- [10] M. Srinivasarao and K. Amundson (unpublished).
- [11] J. L. West, in *Liquid Crystalline Polymers*, edited by R. A. Weiss and C. K. Ober (American Chemical Society, Washington, DC, 1990), Chap. 32.
- [12] J. W. Doane, *Mater. Res. Bull.* **16**, 22 (1991).
- [13] P. S. Drzaic, *Mol. Cryst. Liq. Cryst.* **261**, 383 (1995).
- [14] P. S. Drzaic, in *Liquid Crystal Dispersions* (World Scientific, Singapore, 1995), p. 221.
- [15] Assuming affine deformation of a sphere in shear, the long axis of the deformed sphere can be easily calculated. It will be at 45° from the displacement direction at very low shear, and this angle will decrease toward zero with increasingly strong shear.
- [16] Dr. Frank Allen (private communication).